Impact of sea-ice dynamics on the spatial distribution of diatom resting stages in sediments of the Pacific-Arctic Ocean

Yuri Fukai[1,2], Kohei Matsuno[2,3], Amane Fujiwara[4], Koji Suzuki[1,5], Mindy Richlen[6], Evangeline Fachon[6], Donald M. Anderson[6]

[1] Graduate School of Environmental Science, Hokkaido University, North 10 West 5, Kita-ku, Sapporo, Hokkaido, 060-0810, Japan

[2] Faculty/Graduate School of Fisheries Sciences, Hokkaido University, 3−1−1 Minato-cho, Hakodate, Hokkaido 041-8611, Japan

[3]Arctic Research Center, Hokkaido University, North 21 West 11 Kita-ku, Sapporo, Hokkaido, 001-0021, Japan

[4]Japan Agency for Marine-Earth Science and Technology, 2−15 Natsushima-cho, Yokosuka, Kanagawa, 237-0061, Japan

[5]Faculty of Environmental Earth Science, Hokkaido University, North 10 West 5, Kita-ku, Sapporo, Hokkaido, 060-0810, Japan

[6]Biology Department, Woods Hole Oceanographic Institution, 266 Woods Hole Rd., Woods Hole, MA, 02543, USA

Corresponding author: Yuri Fukai (fukai@ees.hokudai.ac.jp)

Key Points:

- Diatom resting stages in sediments were quantified and explored their relationship to the sea-ice dynamics in the Pacific-Arctic Ocean.
- Diatom assemblage are spatially different depending on the variable timing of the sea-ice retreat and accompanying light conditions.
- Distribution of diatom resting stages had similar geographic features with primary productivity over the Pacific-Arctic Ocean.

Abstract (229 words / up to 250 words)

The Pacific-Arctic Ocean is characterized by seasonal sea-ice, the spatial extent and duration of which varies considerably. In this region, diatoms are the dominant phytoplankton group during spring and summer. To facilitate survival during periods that are less favorable for growth, many diatom species produce resting stages that settle to the seafloor and can serve as a potential inoculum for subsequent blooms. Since diatom assemblage composition is closely related to sea-ice dynamics, detailed studies of biophysical interactions are fundamental to understanding the lower trophic levels of ecosystems in the Pacific-Arctic Ocean. One way to explore this relationship is by comparing the distribution and abundance of diatom resting stages with patterns of sea-ice coverage. In this study, we quantified viable diatom resting stages in sediments in 2018 and explored their relationship to sea-ice extent during the previous winter. Diatom assemblages were clearly dependent on the variable timing of the sea-ice retreat and accompanying light conditions. In areas where sea-ice retreated earlier, open-water species such as *Chaetoceros* spp. and *Thalassiosira* spp. were abundant. In contrast, proportional abundances of *Attheya* spp. and pennate diatom species that are commonly observed in sea-ice were higher in areas where diatoms experienced higher light levels and longer day length in/under the sea-ice due to the late seasonal ice retreat. This study demonstrates that sea-ice dynamics are an important determinant of diatom species composition in the Pacific-Arctic.

Plain Language Summary (197 words / up to 200 words)

The Pacific-Arctic Ocean is characterized by seasonal sea-ice, and when and how long the sea-ice is present varies considerably. In this region, diatoms are the dominant phytoplankton group during spring and summer. Under conditions of unfavorable for growth, many diatom species produce resting stages that are similar to “seeds” of plants, which settle to the seafloor and can reflect the diatom assemblages in the water column. Since what diatom species distribute is closely related to sea-ice dynamics, detailed studies of this relationship are fundamental to understanding the basis of marine ecosystems in the Pacific-Arctic Ocean. In this study, we explored the relationship by comparing the distribution of diatom resting stage assemblages with patterns of sea-ice coverage. Diatom assemblages were dependent on the variable timing of the sea-ice retreat and accompanying light conditions. In areas where sea-ice retreated earlier, open-water species which mainly grow in the water column were abundant, while proportional abundances of ice-associated diatoms that are commonly observed in sea-ice were higher in areas where diatoms experienced favorable light conditions in/under the sea-ice due to the late seasonal ice retreat. This study demonstrates that sea-ice dynamics are an important determinant of diatom composition in the Pacific-Arctic.

1 Introduction

The southeastern Pacific-Arctic ocean extends from the northern Bering Sea to the Chukchi and Beaufort Seas. Within this region, the northern Bering and Chukchi Seas are among the most productive waters in the world (Springer et al., 1996). Phytoplankton are responsible for high primary productivity in the euphotic layer, and most of the cells settle to the seafloor due to

low zooplankton grazing pressure, supporting high benthic biomass with patchy distributions called “benthic hotspots” (Grebmeier et al., 1988, 2006). By contrast, the southwestern Beaufort Sea is low in annual primary productivity (Frost & Lowry, 1984). Here, ice algae production occurs in and under the sea ice, and is followed by phytoplankton blooms (primarily *Chaetoceros* spp.) during the summer retreat of sea-ice (Horner, 1984; Horner & Schrader, 1982). Mean daily water column integrated primary productivity in the southwestern Beaufort Sea is about half of that of the Chukchi Sea, even during peak periods in June and July (Hill et al., 2018). Overall, annual primary production is much higher in the Chukchi shelf than on the Beaufort shelf (Grebmeier et al., 2006).

The Pacific-Arctic is characterized by the presence of seasonal sea-ice, which varies considerably in extent and duration from year to year. The extent of sea-ice has been shown to influence regional phytoplankton assemblages (Neeley et al., 2018), but this relationship is not fully understood. Sea-ice decline has been reported in the Pacific-Arctic ocean (Frey et al., 2018; Grebmeier et al., 2015; Markus et al., 2009), and Arrigo et al. (2008) used satellite observations to show that this decline was associated with significant changes in primary productivity. However, changes in phytoplankton assemblages and particularly in ice-associated assemblages, cannot be evaluated by satellite observations only, necessitating field-based studies to examine the structure of these communities in more detail.

Phytoplankton assemblages during spring and summer blooms in the Pacific-Arctic region are dominated by diatoms (von Quillfeldt, 2000; Sergeeva et al., 2010). In particular, *Chaetoceros socialis s.l.* and *Thalassiosira* spp. are known to form dense blooms in this region (von Quillfeldt, 2000; Sergeeva et al., 2010). The centric diatom *Attheya* spp. is reported to be present in the sea-ice of the Bering Sea and Chukchi Sea (Campbell et al., 2018; Melnikov et al., 2002; von Quillfeldt et al., 2003; Szymanski & Gradinger, 2016; Werner et al., 2007), and pennate diatoms are also known to make up a large proportion of the sea-ice algal community (von Quillfeldt et al., 2003; Szymanski & Gradinger, 2016).

Many diatom species form resting stages under unfavorable growth conditions such as nutrient limitation (Durbin, 1978; Garrison, 1984; McQuoid & Hobson, 1996; Smetacek, 1985), Fe limitation (Sugie & Kuma, 2008) and low light conditions (Hargraves & French, 1983). Resting stages that sink to and accumulate in bottom sediments can germinate and resume growth in response to favorable light levels (Hollibaugh et al., 1981). The ability to form resting

stages is thus an important life cycle strategy for survival under low temperature and light conditions during winter in seasonal sea-ice areas (Tsukazaki et al., 2013, 2018).

The distribution of diatom resting stage assemblages in sediments is thought to reflect the extent and magnitude of past blooms (Itakura et al., 1997; Pitcher, 1990) and can be used to investigate determinants of community structure and bloom dynamics. For example, in the northern Bering Sea, analysis of the diatom resting stage assemblages in sediments showed that diatom assemblages in early spring were dependent upon the timing of the sea-ice retreat: ice-associated diatoms were abundant in 2017 when the sea-ice remained until early April, but open-water diatoms dominated in 2018 when the TSR was approximately two weeks earlier than the previous year (Fukai et al., 2019).

In this study, we enumerated viable diatom resting stages in sediments collected in a broad area across the Pacific-Arctic ocean, from the northern Bering Sea to the Chukchi Sea and the southwestern Beaufort Sea. To this end, we describe the features of diatom resting stage assemblages over these regions, and discuss two hypotheses: 1) the magnitude of diatom resting stage assemblages is correlated with primary production in the water column, and 2) extent and duration of sea-ice during the previous winter determines community structure of diatom resting stage assemblages. In addition, we discuss how observed variations in diatom assemblages may impact organisms at higher trophic levels that rely on diatoms as an important food source.

2 Materials and Methods

2.1 Sea-ice, primary production and daylight hours

To evaluate the sea-ice extent in each region, the Advanced Microwave Scanning Radiometer 2 (AMSR2) standard sea-ice concentration (SIC) product was obtained from the Japan Aerospace Exploration Agency (JAXA) web portal (https :// gport al.jaxa.jp/gpr/) at a 10-km resolution. The timing of the sea-ice retreat (TSR) was defined as the last date when the SIC fell below 20% of the observed annual sea-ice minimum across the study region during the previous summer.

To obtain a continuous primary production time-series, we used Level-3 standard mapped image (9-km resolution) of Aqua-MODIS data downloaded as spectral remote sensing reflectance (R_{rs}) and daily photosynthetically available radiation (PAR) from the Goddard Space

Flight Centre/Distributed Active Archive Centre, NASA. The absorption coefficient for 443 nm ($a_{ph}(443)$) and euphotic zone depth (Z_{eu}) were computed from $R_{rs}(\lambda)$ using Quasi-Analytical Algorithm (QAA) version 5 (Lee et al., 2007, 2009) and daylength (DL) for the study area calculated according to Brock (1981). We then computed the daily euphotic-depth-integrated primary production (PP_{eu}) using $a_{ph}(443)$, Z_{eu}, PAR, and DL as inputs to an absorption-based productivity model (ABPM, (Hirawake et al., 2012). Missing values in $a_{ph}(443)$ and Z_{eu} due to cloud cover were interpolated using their annual medians and hence PP_{eu} was derived for the cloud-covered pixels. From these values we calculated cumulative PP_{eu} (IP_{eu}) and median value of PP_{eu} ($MedP_{eu}$) from TSR to the date of the *in situ* sediment sampling was conducted for each shipboard observation site.

2.2 Sampling

Sediment sampling was conducted in the southeast Pacific-Arctic region (the northern Bering Sea, Chukchi Sea and the southwestern Beaufort Sea; Fig. 1) from 2–12 July 2018 aboard T/S *Oshoro-Maru* of Hokkaido University, and from 9–23 August 2018 and 30 October to 15 November 2018 aboard the U.S. Coast Guard icebreaker *Healy* (*HLY 1801* and *HLY 1803*, respectively). Sediment samples were collected using a multiple corer (*Oshoro-Maru* cruise), a Van Veen Grab sampler, or a HAPS core sampler (*Healy* cruises) at each station. A portion of the 0–1 cm of each sediment core was extruded and stored in darkness at 5˚C for *Oshoro-Maru* samples, and for Healy samples, a portion of the 0–3 cm layer was collected from the grab or the core and stored in air-tight amber jars at 1–4˚C. The sediment samples were stored for more than one month in order to eliminate vegetative cells.

2.3 Quantification of diatom resting stages

The abundance of viable resting stages of diatoms in the sediment samples was analyzed using the most probable number (MPN) method (Imai et al., 1984, 1990). Homogenized wet sediment samples were suspended in Whatman GF/F filtered sterile seawater at a concentration of 0.1 g mL^{-1} (=10^0 dilution), and the subsequent serial tenfold dilutions (10^{-1} to 10^{-6}) were made with modified SWM-3 medium (Chen et al., 1969; Imai et al., 1996). Then 1 mL aliquots of diluted suspensions were inoculated into five replicate wells of disposable tissue culture plates (48 wells). Incubation was carried out at a temperature of 5°C and under white fluorescent light of 50 or 116 µmol photons m^{-2} s^{-1} with a 14 h light:10 h dark photocycle for 10 days. The

appearance of vegetative cells of planktonic diatoms in each well was examined using an inverted optical microscope. The most probable number (MPN for a series of 5 tenfold dilutions) of diatoms in the sediment sample (MPN cells g^{-1} wet sediment) was then calculated according to the statistical table by Throndsen (1978). Note that we used the dataset of Fukai et al. (2019) for the *Oshoro-Maru* expedition.

2.4 Statistical analyses

The diatom resting stage communities were distinguished by cluster analysis. To reduce the bias for abundant species, the cell concentration data (X: MPN cells g^{-1} wet sediment) for each species were transformed to $\sqrt[4]{X}$ prior to cluster analysis (Quinn & Keough, 2002). Dissimilarities between samples were examined using the Bray-Curtis index based on the differences in the species composition. To group the samples, the dissimilarity indices were coupled using hierarchical agglomerative clustering with a complete linkage method (an unweighted pair group method using the arithmetic mean). A Mann-Whitney *U*-test was conducted to evaluate environmental factors (the TSR, IP_{eu}, $MedP_{eu}$, and the growth period of ice-associated assemblages (GP)) between the distinguished groups. The GP was defined as the integrated daylength during the periods with SIC >20% after the daylight exceeded 10 hours, as Gilstad and Sakshaug (1990) indicated that ice-associated assemblages could increase their growth rate when daylight hours exceeded 10 h.

We defined the open-water assemblages as the community with centric diatoms, excluding *Attheya* spp., and the ice-associated assemblages as the community with pennate diatoms and *Attheya* spp., as *Attheya* spp. and pennate diatoms are often reported to be present in the sea-ice (e.g. Campbell et al., 2018; Melnikov et al., 2002; von Quillfeldt et al., 2003; Szymanski & Gradinger, 2016; Werner et al., 2007). Based on this definition, we analyzed the relationships of ice-associated assemblages with the TSR and the GP using Spearman's rank correlation coefficient.

All statistical analyses were conducted using R software (version 3.6.1, R Development Core Team, 2019).

3 Results

3.1 Sea-ice and primary production

The TSR was different among regions (Table 1). The sea-ice retreated from south to north in the northern Bering and the Chukchi Seas, and from west to east in the southwestern Beaufort Sea (Fig.S1 (a)).

The IP_{eu} had a regional feature in which high values were observed in the southern Chukchi Sea and low values in the southwestern Beaufort Sea (Table 1, Fig.S1 (b)). By contrast, $MedP_{eu}$ was locally high in value in some coastal stations in the southwestern Beaufort Sea (Table 1, Fig.S1 (c)).

3.2 Diatom concentrations and species composition

The viable diatom resting stages determined by the MPN method ranged over four orders of magnitude, from 1.2×10^3 to 6.1×10^7 MPN cells g^{-1} wet sediment (Fig. 2). Highest concentrations were found to the south of St. Lawrence Island (3.4×10^6–6.1×10^7 MPN cells g^{-1} wet sediment). In the Chirikov Basin, which extends northwards from St. Lawrence Island to the Bering Strait (DBO2-1, DBO2-4, OS14, OS19, OS20, OS22), diatom concentrations were relatively high (2.8×10^5–3.0×10^6 MPN cells g^{-1} wet sediments). Diatom concentrations near Utqiagvik (DBO5-10) were also relatively high (1.2×10^6 MPN cells g^{-1} wet sediments). In contrast, cell concentrations were lower in samples from the coastal region of the southwestern Beaufort Sea (DBO6-5, PRW-7, PRB-4, PRB-7, KTO-5, MCK-1, MCK-2, MCK-3, MCK-4) (1.2×10^3–7.8×10^3 MPN cells g^{-1} wet sediments). Nineteen genera and twenty species were observed over the study region - 12 genera and 14 species of centric diatoms and 7 genera and 6 species of pennates. Centric diatoms were dominant at almost all stations, although dominant species varied geographically; proportional abundance of *Chaetoceros* spp. and *Thalassiosira* spp. were found in samples collected from the northern Bering Sea and Chukchi Sea, whereas *Attheya* spp. were highest in the southwestern Beaufort Sea (Fig. 3). Pennate diatoms comprised over 50% of the diatom assemblages at some stations (DBO4-4, MCK-1, MCK-2, MCK-3), with highest proportional abundance found in samples from the southwestern Beaufort coastal region (Fig. 3). Total cell concentration in sediments were positively correlated with the cell concentrations of *Chaetoceros* spp. and *Thalassiosira* spp. (Spearman, $\rho = 0.973$, $p < 0.05$) (Fig. S2).

In order to test for seasonal effects, diatom assemblages were compared over time in stations in the northern Bering Sea and Southern Chukchi Sea, which included locations from each sampling period (OS14, 19, 20, 22, 30 by *Oshoro-Maru*, DBO2-1, 2-4, 3-6, 3-8 in *HLY 1801*, and DBO 3-1, 3-5, 3-7 in *HLY 1803)*. With the exception of *Attheya* spp. and *C. debilis*, there were no significant differences in species or genera among these samples (one-way ANOVA, $p > 0.05$).

3.3 Diatom assemblages by cluster analysis

Cluster analysis based on concentrations of diatom resting stages classified the diatom assemblages into two groups (A, B) and four outgroups at 52% and 64% dissimilarity levels (Fig. 4 (a)). Group A was distributed from the northern Bering Sea to the Chukchi Sea near Utqiagvik (Fig. 4 (b)). Cell concentrations in group A were very high (7.9×10^4–1.1×10^7 MPN cells g^{-1} wet sediments, avg = 1.2×10^6 MPN cells g^{-1} wet sediment), and samples in this group with dominated by *Chaetoceros* spp. and *Thalassiosira* spp. (35% and 51%, respectively) (Fig. 4 (c)). Group B included stations from the southwestern Beaufort Sea, where cell concentrations ranged from 3.2×10^3 to 2.1×10^5 MPN cells g^{-1} wet sediment (avg = 5.8×10^4 MPN cells g^{-1} wet sediment) and *Attheya* spp. was dominant (47%) (Fig. 4 (b), (c)). All stations from the easternmost transect in the study region (MCK) were classified as outgroups (Fig. 4 (b), (c)).

3.4 Relationships with environmental factors

Environmental factors differed between samples comprising diatom groups A and B. The TSR was significantly later at the group B locations compared to group A (*U*-test, $p < 0.05$) (Fig.5 a), and the GP was significantly longer at group B locations than group A (*U*-test, $p < 0.05$) (Fig. 5 b). The swithing between the two diatom groups occurred around 200 Julian day of the TSR and approximately 2500 hours of the GP (Fig. 5 a, b, Fig.6). By contrast, the IP_{eu}, $MedP_{eu}$ and the sampling depth were not significantly different between groups (*U*-test, $p > 0.05$) (Fig.5 c, d, e).

In addition, the TSR and the GP were significantly positively correlated with the proportion of pennate diatoms and *Attheya* spp. ($\rho = 0.63$ and 0.29, respectively, $p < 0.05$) (Fig.6). Here, we supposed the community of the pennate diatoms and *Attheya* spp. as the ice-associated assemblages, because the pennate diatoms and *Attheya* spp. are predominant in sea-ice

(e.g. Campbell et al., 2018; Melnikov et al., 2002; von Quillfeldt et al., 2003; Szymanski & Gradinger, 2016; Werner et al., 2007).

4 Discussion

This study examined the distribution and abundance of diatom resting stages in the Pacific Arctic sediments and demonstrated a strong correlation with the timing of sea ice retreat and the growth period of ice-associated assemblages. Details regarding spatial community dynamics and relationships between diatom assemblages and TSR, GP, and environmental parameters are discussed below.

4.1 Distribution of diatom resting stages and the relationships with primary production in the Pacific-Arctic Region

Cell concentrations of diatom resting stages exhibited geographic variability that roughly corresponded with levels of primary production previously reported in the region. However, primary production values estimated by satellite in this study did not have any statistically significant relationships with diatom resting stage assemblages.

This study found high concentrations of diatom resting stages in the northern Bering Sea and the Chukchi Sea (avg = 3.1×10^6 MPN cells g^{-1} wet sediments), but low concentrations (avg = 6.2×10^4 MPN cells g^{-1} wet sediments) in the southwestern Beaufort Sea. Prior studies of primary productivity within the study region documented high annual water-column integrated primary production in the northern Bering and Chukchi Seas and low productivity in the western Beaufort Sea (Grebmeier et al., 2006; Hill et al., 2018). Since the distribution of diatom resting stages is thought to reflect primary productivity in the water column (Imai et al., 1990; Itakura et al., 1997; Pitcher, 1990), the resting stage distribution over the Pacific-Arctic region can be used as a proxy for productivity in the water column in that region. In the western Arctic Ocean, grazing rates of micro- and meso-zooplankton are lower than rates measured in another Arctic system, the Barents Sea; consequently, grazing impacts to chlorophyll standing stock and primary production are low (Campbell et al., 2009; Sherr et al., 2009). Under low grazing pressure across the shallow shelves in the Pacific-Arctic region, higher proportions of diatom resting cells would settle from the water column to the seafloor, and the distribution of resting stage assemblages would reflect the high levels of water-column primary production. While we

were not able to strictly quantify primary production at each station, this assessment of diatom assemblages in sediments allows us to characterize broad features of primary productivity over a wide region in the Pacific-Arctic Ocean.

We considered the impact that variable sampling times may have had upon the assemblages observed in this study. The sediments collected for this study were obtained over several different time periods (2–12 July 2018, 9–23 August 2018, and 30 October to 15 November 2018), and it is possible that the community structure changed from summer to fall. However, there were no significant differences in species or genera except for *Attheya* spp. and *C. debilis* between samples at replicated stations in the northern Bering Sea and Southern Chukchi Sea, where sampling was conducted over multiple time periods. Dissimilarity among almost all the samples was less than 40%, and they were also grouped in the cluster analysis. Thus, differences over sampling periods appeared to be almost negligible in this study.

4.2 The relationship of diatom resting stage assemblages with the TSR and the GP

Prior investigators have shown that the magnitude and composition of diatom assemblages in the Arctic spring bloom are influenced by the presence of the sea-ice and the timing of the sea-ice retreat (Fujiwara et al., 2016; Fukai et al., 2019; Neeley et al., 2018). In this study, the distribution of diatom resting stage assemblages were clearly related to spatial differences in the TSR. In locations where the ice retreat was early, such as the northern Bering and the Chukchi Seas, *Chaetoceros* spp. including *C. socialis s.l.* and *Thalassiosira* spp. were dominant in sediments (*C. socialis s.l.*: 0.36–93.1%, *Chaetoceros* spp.: 0.76–93.6%, *Thalassiosira* spp.: 2.0–96.4%). Because they are known to form dense spring blooms in these regions (von Quillfeldt, 2000; Sergeeva et al., 2010), these data indicate that diatom resting stages were formed and settled to the seafloor after spring blooms of *Chaetoceros* spp. and *Thalassiosira* spp. in the northern Bering Sea and the Chukchi Sea. In addition, the positive correlation between *Chaetoceros* spp. and *Thalassiosira* spp. cell concentrations with total cell concentrations indicates that where the TSR was early and the open-water period was long, large diatom blooms of *Chaetoceros* spp. and *Thalassiosira* spp. produced high concentrations of resting stage cells (Fujiwara et al., 2016; Fukai et al., 2019).

The TSR had also an effect on the diatom community composition, especially the proportion of ice-associated diatoms in diatom assemblages. Here, we defined ice-associated diatoms as “pennate diatoms and *Attheya* spp.” because pennate diatoms comprise a large

proportion of the sea-ice algal community (von Quillfeldt et al., 2003; Szymanski & Gradinger, 2016), and *Attheya* spp. was often reported in the sea-ice of the Bering Sea and Chukchi Sea (Campbell et al., 2018; Melnikov et al., 2002; von Quillfeldt et al., 2003; Szymanski & Gradinger, 2016; Werner et al., 2007). Under this definition, diatom assemblages in the southwestern Beaufort Sea, where the TSR was late, were dominated by ice-associated species (Groups B and outgroups in the transect MCK), again demonstrating that sea-ice is a driver of benthic diatom community structure. In addition, the prevalence of ice-associated species was positively correlated with the TSR, suggesting that the proportion of ice algae in diatom assemblages is higher when sea-ice persists. This is likely due in part to their ability to sustain growth under low light levels (< 1 μmol photon s^{-1} m^{-2}) (Cota & Smith, 1991; Mock & Gradinger, 1999); notably, Tsukazaki et al. (2018) demonstrated that the centric genus *Attheya* spp. could survive in dark for more than six months, and thus can withstand low light conditions in the Arctic. It is possible that this study underestimated the concentrations of pennate diatoms in sediments compared with *Attheya* spp. and other centric diatoms, as few marine pennate diatoms are known to form resting stages, while many centric diatoms do (McQuoid & Hobson, 1996), and the fate of the pennate diatoms in sediment is largely unknown. Despite this potential bias, these data indicate that the proportion of ice-associated species was higher where the TSR occurred later. In addition, interestingly, a spatial change from the assemblage dominated by open-water species to that with high proportion of ice-associated diatoms would have occurred around 200 Julian day (mid-July) of the TSR. This may indicate that swithing of dominant diatom group in spring blooms may occur based on this TSR parameter.

For ice-associated assemblages in the surface sediments, the length of the growth period during which algae receive sufficient light before the TSR is important (Fukai et al., 2019). We defined the growth period of the ice-associated assemblages (GP) as the integrated daylength during the periods with SIC > 20% after the daylight hours exceed 10 hours, the threshold for increased growth in ice-associated assemblages (Gilstad & Sakshaug, 1990). The proportional abundance of ice-associated diatoms was significantly higher when GP was longer, suggesting that photoperiod during sea-ice presence is another important driver of diatom community structure (Cota & Home, 1989; Gosselin et al., 1990; Smith et al., 1988). In addition, a GP boundary of 2500 hours may be an important parameter for the distribution of ice-associated

assemblages. Future efforts to evaluate and predict diatom assemblages should consider both the TSR and the GP.

4.3 Connecting diatom distribution to higher trophic levels

The diatom assemblages had clear relationships with the TSR and the GP. In the northern Bering Sea, the early timing of the sea-ice retreat and subsequent changes in diatom assemblages in the water column and the sediment was reported in 2018 (Fukai et al., 2019, 2020). This indicates that the recent drastic reduction of sea-ice in the Pacific-Arctic region may induce a shift in diatom assemblages from relative dominance of ice-associated species to open-water species.

Changes in diatom species composition will perturb prey environments of higher trophic level organisms. The distribution and composition of diatom species in this study seemed to be associated with the zooplankton feeding environment in the Pacific-Arctic region. The spatial trend of diatom resting stage concentrations exhibited a similar gradient to zooplankton $\delta^{13}C$ values showed by Pomerleau et al. (2014), which reported values that were more enriched in the western Bering Strait and less enriched on the Beaufort shelf. Typically, zooplankton that feed on fast-growing diatoms (e.g. *Chaetoceros* spp. and *Thalassiosira* spp.) are enriched with ^{13}C (Perry et al., 2011). The inflow of nutrient rich Anadyr waters from the western Bering Strait is known to fuel huge blooms of *Chaetoceros* spp. and *Thalassiosira* spp. (Danielson et al., 2017; Sergeeva et al., 2010), explaining the high concentrations of these species in sediments of the northern Bering and the Chukchi Seas reported here. In addition, regions of high diatom resting stage concentrations roughly corresponded to benthic hotspots, which include waters to the south of St. Lawrence Island, the Chirikov Basin, the southeastern Chukchi Sea and the northeastern Chukchi Sea (Grebmeier et al., 2015). In these regions, ice algae and phytoplankton are more important food resources for benthic communities than benthic microalgae (Grebmeier et al., 2015), and diatoms are particularly valuable taxa because they are rich in polyunsaturated fatty acids (PUFAs) (Brown et al., 1997). Furthermore, Wang et al. (2016) analyzed the blubber fatty acid composition and stable carbon isotope ratios of ice seals, who feed on pelagic and benthic fishes, in the northern Bering and the southern Chukchi Seas to show that ice algae contributed more to their food web in the cold years than in warm years. Therefore, changes in diatom assemblages caused by sea-ice dynamics will directly influence zooplankton and benthos production, with indirect effects upon higher trophic levels.

5 Conclusions

This study demonstrated that the distribution and community composition of diatom resting stages in the southeastern Pacific-Arctic region was significantly influenced by the presence of sea-ice and the light environment. We were also able to capture general features of primary productivity over the wider Pacific-Arctic region by assessing diatoms in sediments, although no clear relationship with primary productivity estimated by satellite observations was found. Important drivers of the diatom assemblages, the TSR and the GP, significantly influenced the composition of diatoms in sediments. In particular, diatom assemblages changed spatially from open-water species dominated composition to high proportion of ice-associated diatoms in the region where the TSR occurred after mid-July (around 200 Julian day) and the GP was over 2500 hours. This result may indicate that shift to earlier TSR in the future induce not only change in diatom bloom timing but also change in the compotion of diatom assemblages forming the spring bloom. The distribution of diatom resting stages is a valuable approach for investigating the diatom community, particularly on the Arctic shelves where it is logistically challenging to characterize the rapid seasonal succession in community composition that occurs across this remote and dynamic geographic region. Moreover, this approach provides species-level resolution lacking in satellite observations, providing a more robust assessment of the ecosystem implications of community changes. As for the marine ecosystems, it is interesting that the distribution of diatom resting stages corresponded spatially with the benthic hot spots and the feeding environment of zooplankton. Based on this research, it is clear that future changes in sea-ice extent and duration will impact diatom communities, and that resulting fluctuations in primary productivity and community structure will impact other components of Arctic marine ecosystems.

Acknowledgments

We thank the captain, officers, crews and researchers on board the U.S. Coast Guard icebreaker *Healy* and the T/S *Oshoro-Maru*, Hokkaido University for their great efforts during the field sampling. We also acknowledge the JAXA Earth Observation Research Center and NASA/GSFC for providing satellite data. This work was conducted by the Arctic Challenge for Sustainability (ArCS) project, Arctic Challenge for Sustainability II (ArCSII) project and ArCS program for overseas visits by young researchers. In addition, this work was partly

supported by the Japan Society for the Promotion of Science (JSPS) KAKENHI Grant Number JP20J20410. We thank Anderson laboratory members for their support of our study at WHOI, and also thank Robert Pickart, Leah McRaven, and Jacqueline Grebmeier for their support and assistance on the Healy cruises. Funding for DA, EF, and MR was provided by the NOAA Arctic Research Program through the Cooperative Institute for the North Atlantic Region (CINAR Award NA14OAR4320158), by the NOAA ECOHAB Program (NA20NOS4780195) and by the National Science Foundation Office of Polar Programs (OPP-1823002). The data reported in this paper have been deposited in the data archive site of Hokkaido University, http://hdl.handle.net/2115/80394

References

Arrigo, K. R., van Dijken, G., & Pabi, S. (2008). Impact of a shrinking Arctic ice cover on marine primary production. *Geophysical Research Letters*, *35*(19), L19603. https://doi.org/10.1029/2008GL035028

Brock, T. D. (1981). Calculating solar radiation for ecological studies. *Ecological Modelling*, *14*(1), 1–19. https://doi.org/10.1016/0304-3800(81)90011-9

Brown, M. R., Jeffrey, S. W., Volkman, J. K., & Dunstan, G. A. (1997). Nutritional properties of microalgae for mariculture. *Aquaculture*, *151*(1–4), 315–331. https://doi.org/10.1016/S0044-8486(96)01501-3

Campbell, K., Mundy, C. J., Belzile, C., Delaforge, A., & Rysgaard, S. (2018). Seasonal dynamics of algal and bacterial communities in Arctic sea ice under variable snow cover. *Polar Biology*, *41*(1), 41–58. https://doi.org/10.1007/s00300-017-2168-2

Campbell, R. G., Sherr, E. B., Ashjian, C. J., Plourde, S., Sherr, B. F., Hill, V., & Stockwell, D. A. (2009). Mesozooplankton prey preference and grazing impact in the western Arctic Ocean. *Deep Sea Research Part II: Topical Studies in Oceanography*, *56*(17), 1274–1289. https://doi.org/10.1016/j.dsr2.2008.10.027

Cota, G. F., & Home, E. (1989). Physical control of arctic ice algal production. *Marine Ecology Progress Series*, *52*, 111–121. https://doi.org/10.3354/meps052111

Cota, G. F., & Smith, R. E. H. (1991). Ecology of bottom ice algae: II. Dynamics, distributions and productivity. *Journal of Marine Systems*, *2*(3), 279–295. https://doi.org/10.1016/0924-7963(91)90037-U

Danielson, S. L., Eisner, L., Ladd, C., Mordy, C., Sousa, L., & Weingartner, T. J. (2017). A comparison between late summer 2012 and 2013 water masses, macronutrients, and phytoplankton standing crops in the northern Bering and Chukchi Seas. *Deep Sea Research Part II: Topical Studies in Oceanography*, *135*, 7–26. https://doi.org/10.1016/j.dsr2.2016.05.024

Durbin, E. G. (1978). Aspects of the biology of resting spores of Thalassiosira nordenskioeldii and Detonula confervacea. *Marine Biology*, *45*(1), 31–37. https://doi.org/10.1007/BF00388975

Frey, K. E., Comiso, J. C., Cooper, L. W., Grebmeier, J. M., & Stock, L. V. (2018). Arctic Ocean Primary Productivity: The Response of Marine Algae to Climate Warming and Sea Ice Decline, 7.

Frost, K. J., & Lowry, L. F. (1984). Trophic relationships of vertebrate consumers in the Alaskan Beaufort Sea. In P. W. Barnes, D. M. Schell, & E. Reimnitz, *The Alaskan Beaufort Sea: Ecosystems and Environments* (pp. 381–401). Florida: Academic Press.

Fujiwara, A., Hirawake, T., Suzuki, K., Eisner, L., Imai, I., Nishino, S., et al. (2016). Influence of timing of sea ice retreat on phytoplankton size during marginal ice zone bloom period on the Chukchi and Bering shelves. *Biogeosciences*, *13*(1), 115–131. https://doi.org/10.5194/bg-13-115-2016

Fukai, Y., Matsuno, K., Fujiwara, A., & Yamaguchi, A. (2019). The community composition of diatom resting stages in sediments of the northern Bering Sea in 2017 and 2018: the

relationship to the interannual changes in the extent of the sea ice. *Polar Biology*, *42*(10), 1915–1922. https://doi.org/10.1007/s00300-019-02552-x

Fukai, Y., Abe, Y., Matsuno, K., & Yamaguchi, A. (2020). Spatial changes in the summer diatom community of the northern Bering Sea in 2017 and 2018. *Deep Sea Research Part II: Topical Studies in Oceanography*, *181–182*, 104903. https://doi.org/10.1016/j.dsr2.2020.104903

Garrison, D. L. (1984). Chapter 1, Planktonic Diatoms. *Marine Plankton Life Cycle Strategies*, 1–17.

Gilstad, M., & Sakshaug, E. (1990). Growth rates of ten diatom species from the Barents Sea at different irradiances and day lengths. *Marine Ecology Progress Series*, *64*, 169–173. https://doi.org/10.3354/meps064169

Gosselin, M., Legendre, L., Therriault, J.-C., & Demers, S. (1990). Light and Nutrient Limitation of Sea-Ice Microalgae (hudson Bay, Canadian Arctic)1. *Journal of Phycology*, *26*(2), 220–232. https://doi.org/10.1111/j.0022-3646.1990.00220.x

Grebmeier, J. M., McRoy, C., & Feder, H. (1988). Pelagic-benthic coupling on the shelf of the northern Bering and Chukchi Seas. I. Food supply source and benthic bio-mass. *Marine Ecology Progress Series*, *48*, 57–67. https://doi.org/10.3354/meps048057

Grebmeier, J. M., Cooper, L. W., Feder, H. M., & Sirenko, B. I. (2006). Ecosystem dynamics of the Pacific-influenced Northern Bering and Chukchi Seas in the Amerasian Arctic. *Progress in Oceanography*, *71*(2–4), 331–361. https://doi.org/10.1016/j.pocean.2006.10.001

Grebmeier, J. M., Bluhm, B. A., Cooper, L. W., Danielson, S. L., Arrigo, K. R., Blanchard, A. L., et al. (2015). Ecosystem characteristics and processes facilitating persistent macrobenthic

biomass hotspots and associated benthivory in the Pacific Arctic. *Progress in Oceanography*, *136*, 92–114. https://doi.org/10.1016/j.pocean.2015.05.006

Hargraves, P. E., & French, F. W. (1983). Diatom resting spore: significance and strategies. In G. A. Fryxell, *Survival Strategies of the Algae* (pp. 49–68). New York: Cambridge University Press.

Hill, V., Ardyna, M., Lee, S. H., & Varela, D. E. (2018). Decadal trends in phytoplankton production in the Pacific Arctic Region from 1950 to 2012. *Deep Sea Research Part II: Topical Studies in Oceanography*, *152*, 82–94. https://doi.org/10.1016/j.dsr2.2016.12.015

Hirawake, T., Shinmyo, K., Fujiwara, A., & Saitoh, S. (2012). Satellite remote sensing of primary productivity in the Bering and Chukchi Seas using an absorption-based approach. *ICES Journal of Marine Science*, *69*(7), 1194–1204. https://doi.org/10.1093/icesjms/fss111

Hollibaugh, J. T., Seibert, D. L. R., & Thomas, W. H. (1981). Observations on the Survival and Germination of Resting Spores of Three Chaetoceros (bacillariophyceae) Species1,2. *Journal of Phycology*, *17*(1), 1–9. https://doi.org/10.1111/j.1529-8817.1981.tb00812.x

Horner, R. (1984). Phytoplankton abundance, chlorophyll a, and primary production in the western Beaufort Sea. In P. W. Barnes, D. M. Schell, & E. Reimnitz, *The Alaskan Beaufort Sea: Ecosystems and Environments* (pp. 295–310). Florida: Academic Press.

Horner, R., & Schrader, G. C. (1982). Relative Contributions of Ice Algae, Phytoplankton, and Benthic Microalgae to Primary Production in Nearshore Regions of the Beaufort Sea. *ARCTIC*, *35*(4), 485–503. https://doi.org/10.14430/arctic2356

Imai, I., Itoh, K., & Anraku, M. (1984). Extinction Dilution Method for Enumeration of Dormant Cells of Red Tide Organisms in Marine Sediments. *Bulletin of Plankton Society of Japan*,

312, 123–124.

Imai, I., Itakura, S., & Itoh, K. (1990). Distribution of diatom resting cells in sediments of Harima-Nada and northern Hiroshima Bay, the Seto Island Sea, Japan. *Bulletin on coastal oceanography*, *28*(1), 75–84. https://doi.org/10.32142/engankaiyo.28.1_75

Itakura, S., Imai, I., & Itoh, K. (1997). "Seed bank" of coastal planktonic diatoms in bottom sediments of Hiroshima Bay, Seto Inland Sea, Japan. *Marine Biology*, *128*(3), 497–508. https://doi.org/10.1007/s002270050116

Lee, Z., Weidemann, A., Kindle, J., Arnone, R., Carder, K. L., & Davis, C. (2007). Euphotic zone depth: Its derivation and implication to ocean-color remote sensing. *Journal of Geophysical Research: Oceans*, *112*(C3). https://doi.org/10.1029/2006JC003802

Lee, Z., Lubac, B., Werdell, J., & Arnone, R. (2009, January 1). An Update of the Quasi-Analytical Algorithm (QAA_v5). Retrieved January 6, 2021, from http://www.ioccg.org/groups/software.html

Markus, T., Stroeve, J. C., & Miller, J. (2009). Recent changes in Arctic sea ice melt onset, freezeup, and melt season length. *Journal of Geophysical Research: Oceans*, *114*(C12). https://doi.org/10.1029/2009JC005436

McQuoid, M. R., & Hobson, L. A. (1996). Diatom resting stages. *Journal of Phycology*, *32*(6), 889–902. https://doi.org/10.1111/j.0022-3646.1996.00889.x

Melnikov, I. A., Kolosova, E. G., Welch, H. E., & Zhitina, L. S. (2002). Sea ice biological communities and nutrient dynamics in the Canada Basin of the Arctic Ocean. *Deep Sea Research Part I: Oceanographic Research Papers*, *49*(9), 1623–1649. https://doi.org/10.1016/S0967-0637(02)00042-0

Mock, T., & Gradinger, R. (1999). Determination of Arctic ice algal production with a new in

situ incubation technique. *Marine Ecology Progress Series*, *177*, 15–26. https://doi.org/10.3354/meps177015

Neeley, A. R., Harris, L. A., & Frey, K. E. (2018). Unraveling Phytoplankton Community Dynamics in the Northern Chukchi Sea Under Sea-Ice-Covered and Sea-Ice-Free Conditions. *Geophysical Research Letters*, *45*(15), 7663–7671. https://doi.org/10.1029/2018GL077684

Perry, R. I., Thompson, P. A., Mackas, D. L., Harrison, P. J., & Yelland, D. R. (2011). Stable carbon isotopes as pelagic food web tracers in adjacent shelf and slope regions off British Columbia, Canada. *Canadian Journal of Fisheries and Aquatic Sciences*. https://doi.org/10.1139/f99-194

Pitcher, G. C. (1990). Phytoplankton seed populations of the Cape Peninsula upwelling plume, with particular reference to resting spores of Chaetoceros (bacillariophyceae) and their role in seeding upwelling waters. *Estuarine, Coastal and Shelf Science*, *31*(3), 283–301. https://doi.org/10.1016/0272-7714(90)90105-Z

Pomerleau, C., Nelson, R. J., Hunt, B. P. V., Sastri, A. R., & Williams, W. J. (2014). Spatial patterns in zooplankton communities and stable isotope ratios (δ13C and δ15N) in relation to oceanographic conditions in the sub-Arctic Pacific and western Arctic regions during the summer of 2008. *Journal of Plankton Research*, *36*(3), 757–775. https://doi.org/10.1093/plankt/fbt129

von Quillfeldt, C. H. (2000). Common Diatom Species in Arctic Spring Blooms: Their Distribution and Abundance. *Botanica Marina*, *43*(6), 499–516. https://doi.org/10.1515/BOT.2000.050

von Quillfeldt, C. H., Ambrose, W. G., & Clough, L. M. (2003). High number of diatom species

546 in first-year ice from the Chukchi Sea. *Polar Biology*, *26*(12), 806–818.
547 https://doi.org/10.1007/s00300-003-0549-1
548 Quinn, G. P., & Keough, M. J. (2002). *Experimental Design and Data Analysis for Biologists*.
549 New York: Cambridge University Press.
550 Sergeeva, V. M., Sukhanova, I. N., Flint, M. V., Pautova, L. A., Grebmeier, J. M., & Cooper, L.
551 W. (2010). Phytoplankton community in the Western Arctic in July–August 2003.
552 *Oceanology*, *50*(2), 184–197. https://doi.org/10.1134/S0001437010020049
553 Sherr, E. B., Sherr, B. F., & Hartz, A. J. (2009). Microzooplankton grazing impact in the Western
554 Arctic Ocean. *Deep Sea Research Part II: Topical Studies in Oceanography*, *56*(17),
555 1264–1273. https://doi.org/10.1016/j.dsr2.2008.10.036
556 Smetacek, V. S. (1985). Role of sinking in diatom life-history cycles: ecological, evolutionary
557 and geological significance. *Marine Biology*, *84*(3), 239–251.
558 https://doi.org/10.1007/BF00392493
559 Smith, W. O., Keene, N. K., & Comiso, J. C. (1988). Interannual Variability in Estimated
560 Primary Productivity of the Antarctic Marginal Ice Zone. In D. Sahrhage (Ed.), *Antarctic*
561 *Ocean and Resources Variability* (pp. 131–139). Berlin, Heidelberg: Springer.
562 https://doi.org/10.1007/978-3-642-73724-4_10
563 Springer, A. M., McROY, C. P., & Flint, M. V. (1996). The Bering Sea Green Belt: shelf-edge
564 processes and ecosystem production. *Fisheries Oceanography*, *5*(3–4), 205–223.
565 https://doi.org/10.1111/j.1365-2419.1996.tb00118.x
566 Sugie, K., & Kuma, K. (2008). Resting spore formation in the marine diatom Thalassiosira
567 nordenskioeldii under iron- and nitrogen-limited conditions. *Journal of Plankton*
568 *Research*, *30*(11), 1245–1255. https://doi.org/10.1093/plankt/fbn080

569 Szymanski, A., & Gradinger, R. (2016). The diversity, abundance and fate of ice algae and
570 phytoplankton in the Bering Sea. *Polar Biology*, *39*(2), 309–325.
571 https://doi.org/10.1007/s00300-015-1783-z
572 Throndsen, J. (1978). The dilution-culture method. In A. Sournia, *Phytoplankton Manual* (pp.
573 218–224). Paris: Unesco.
574 Tsukazaki, C., Ishii, K.-I., Saito, R., Matsuno, K., Yamaguchi, A., & Imai, I. (2013). Distribution
575 of viable diatom resting stage cells in bottom sediments of the eastern Bering Sea shelf.
576 *Deep Sea Research Part II: Topical Studies in Oceanography*, *94*, 22–30.
577 https://doi.org/10.1016/j.dsr2.2013.03.020
578 Tsukazaki, C., Ishii, K.-I., Matsuno, K., Yamaguchi, A., & Imai, I. (2018). Distribution of viable
579 resting stage cells of diatoms in sediments and water columns of the Chukchi Sea, Arctic
580 Ocean. *Phycologia*, *57*(4), 440–452. https://doi.org/10.2216/16-108.1
581 Wang, S. W., Springer, A. M., Budge, S. M., Horstmann, L., Quakenbush, L. T., & Wooller, M. J.
582 (2016). Carbon sources and trophic relationships of ice seals during recent environmental
583 shifts in the Bering Sea. *Ecological Applications*, *26*(3), 830–845.
584 https://doi.org/10.1890/14-2421
585 Werner, I., Ikävalko, J., & Schünemann, H. (2007). Sea-ice algae in Arctic pack ice during late
586 winter. *Polar Biology*, *30*(11), 1493–1504. https://doi.org/10.1007/s00300-007-0310-2å

587

Figure and Table legends

Figure 1. Locations of the sediment sampling in the northern Bering Sea, Chukchi Sea, and Beaufort Sea in 2018. Color contours indicate the timing of the sea-ice retreat (rainbow contour) and the bottom depth (blue contour). Abbreviations indicate the transect names during Healy cruises 1801 and 1803.

Figure 2. Horizontal distribution of diatom resting stages in the north Bering, Chukchi and Beaufort Seas in 2018.

Figure 3. Cell concentrations and species composition of diatom resting stages in the northern Bering, Chukchi and Beaufort Seas in 2018.

Figure 4. (a) Spatial distribution of diatom resting stage communities by group. (b) Species composition and cell concentrations in each group.

Figure 5. Comparison of environmental factors between diatom resting stage groups. (a) the timing of the sea-ice retreat (TSR). (b) the growth period of ice-associated assemblages (GP). (c) the daily cumulative euphotic-depth-integrated primary production (IP_{eu}). (d) the median values of primary productivity from the TSR to the observation date ($MedP_{eu}$). (e) the bottom depth of sampling station.

Figure 6. Relationships between the proportion of the ice-associated species (*Attheya* spp. and pennate diatoms) in MPN and the TSR (a), and the GP (b). Each color indicate the diatom groups (pink: group A, green: group B, and gray: out groups).

Figure S1. Horizontal values of the integrated primary productivity from the TSR to the observation date (IP_{eu}) (a), the median values of primary productivity from the TSR to the observation date ($MedP_{eu}$) (b), and the observation date (c).

Figure S2. The relationship between the total cell concentrations and, *Chaetoceros* spp. and *Thalassiosira* spp. in MPN.

Table1. Locations of sediment sampling stations in the Bering, Chukchi, and Beaufort Seas from July to November in 2018. In sample type column, “core” and “Van Veen” indicate that the samples were collected by multiple corer and Van Veen grab sampler, respectively. The timing of sea ice retreat (TSR) indicates the last date when the sea ice concentration falls below 20%, prior to observed annual sea ice minimum across the study region during summer. IPeu and MedPeu indicate daily integrated value and median value of primary production from TSR to the date of the *in situ* sediment sampling was conducted. The growth period of the ice-associated assemblages (GP) indicates the integrated daylength during the periods with SIC > 20% after the daylight hours exceed 10 hours.

Figure.

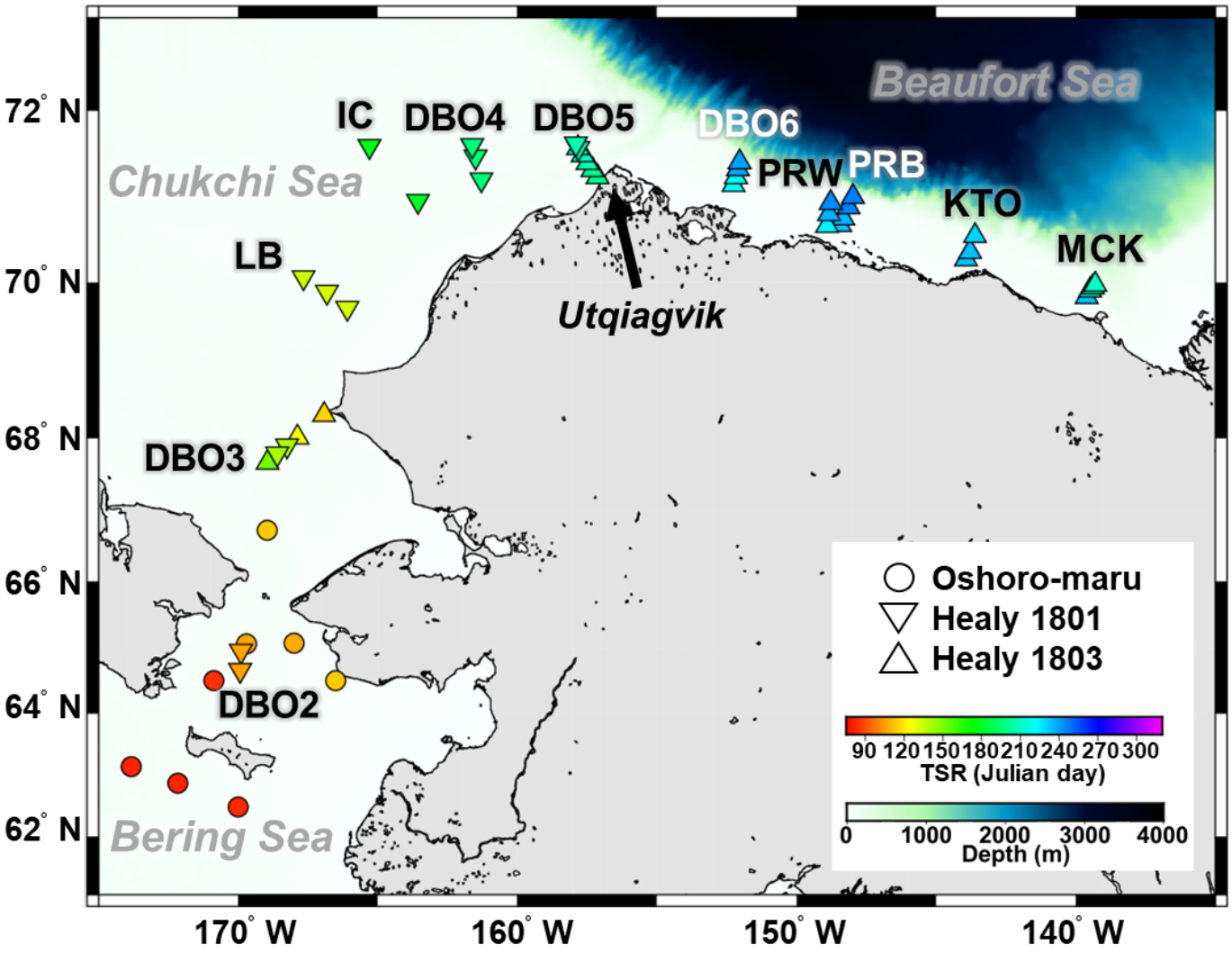

Fig. 1. Locations of the sediment sampling in the northern Bering Sea, Chukchi Sea, and Beaufort Sea in 2018. Color contours indicate the timing of the sea-ice retreat (rainbow contour) and the bottom depth (blue contour). Abbreviations indicate the transect names during Healy cruises 1801 and 1803.

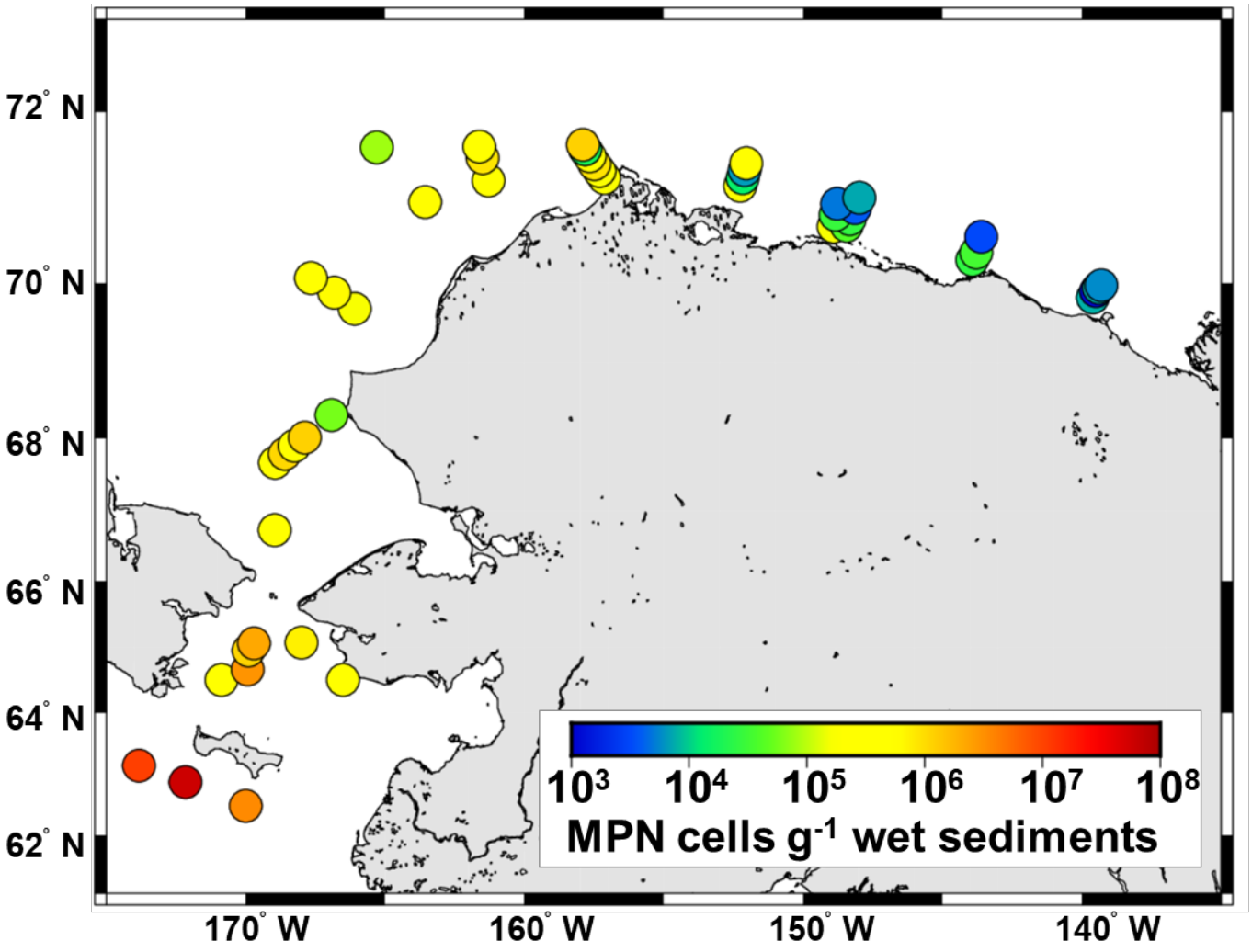

Fig. 2. Horizontal distribution of diatom resting stages in the north Bering, Chukchi and Beaufort Seas in 2018.

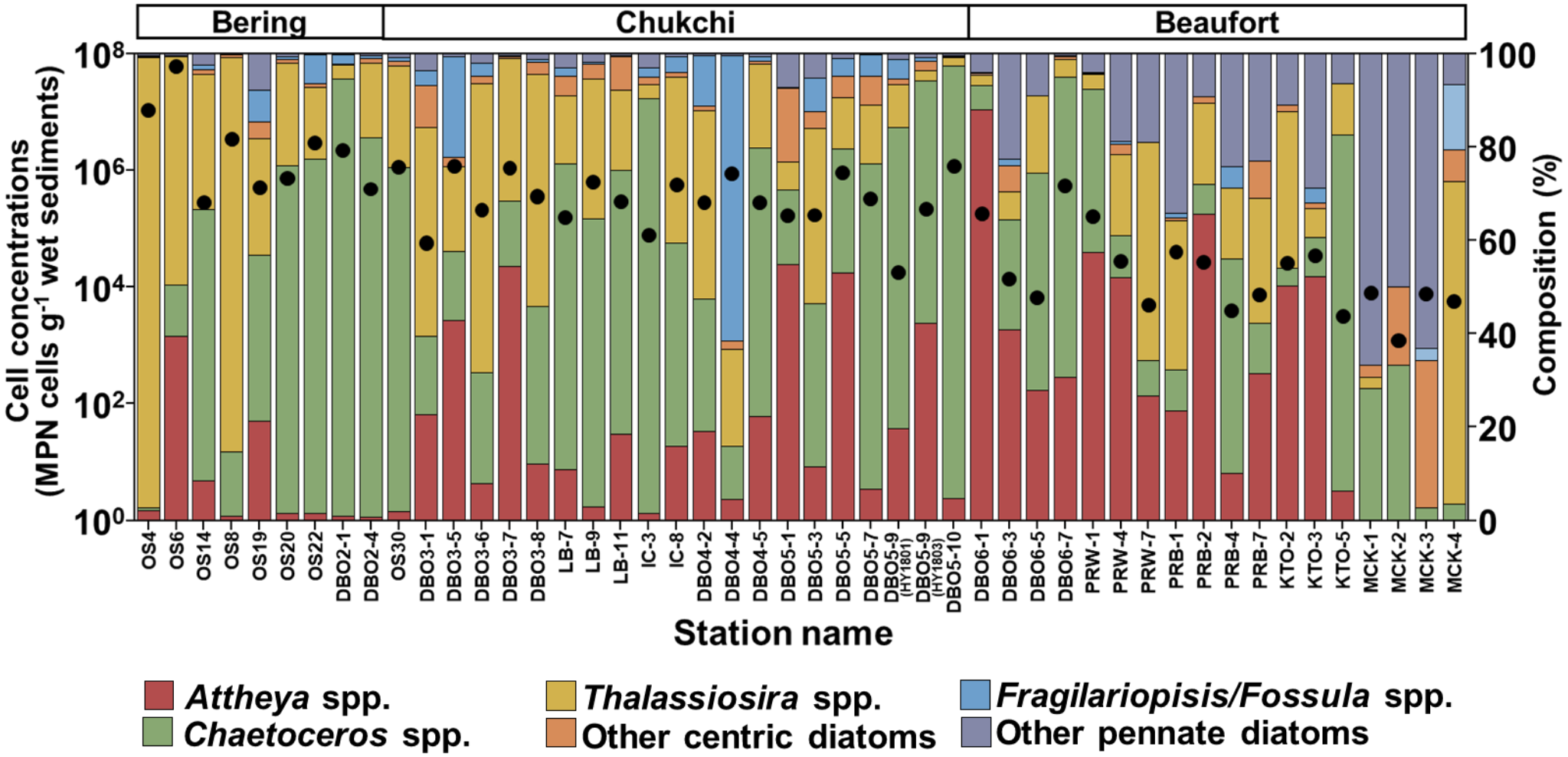

Fig. 3. Cell concentrations and species composition of diatom resting stages in the northern Bering, Chukchi and Beaufort Seas in 2018.

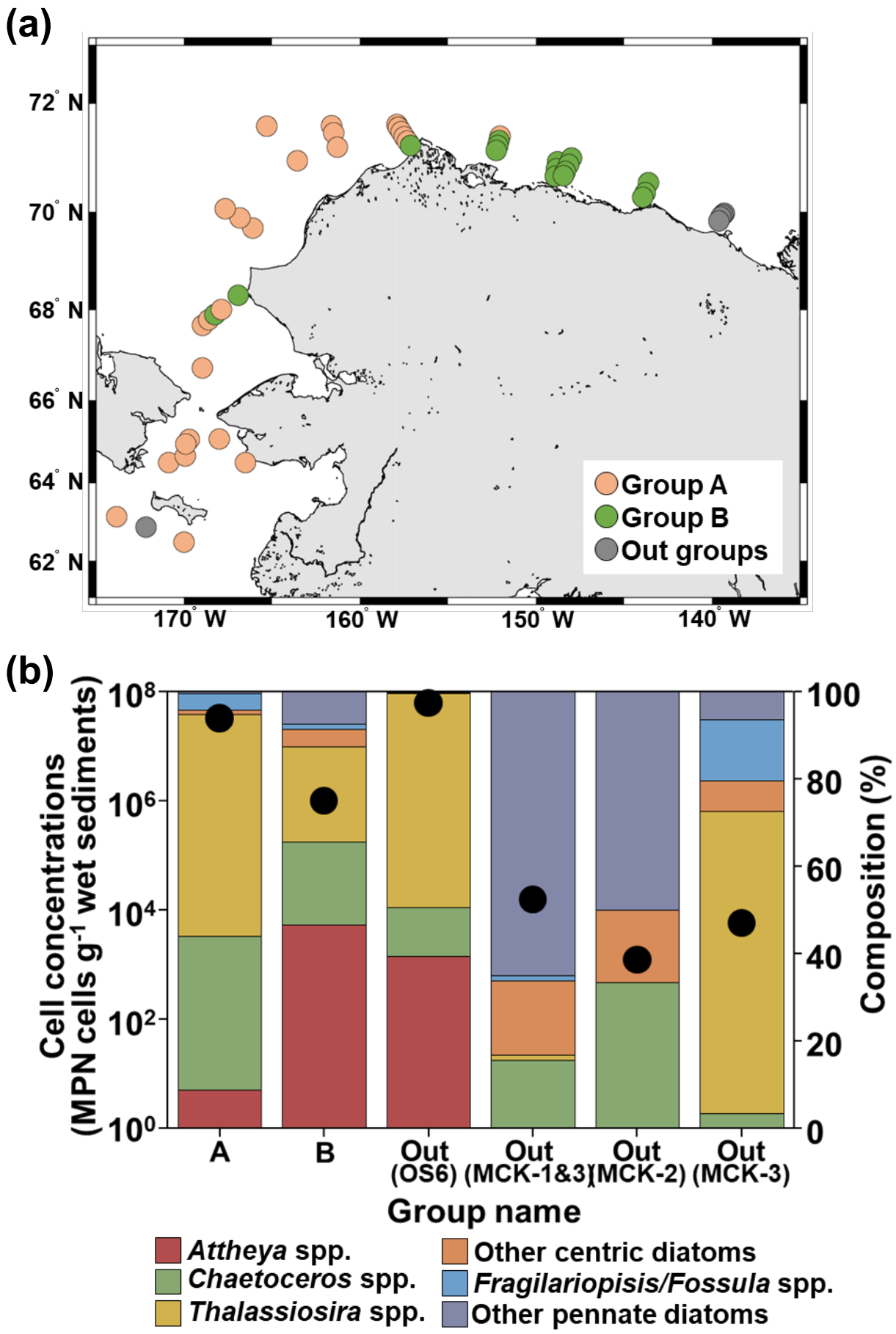

Fig. 4. (a) Spatial distribution of diatom resting stages communities by group. (b) Species composition and cell concentrations in each group.

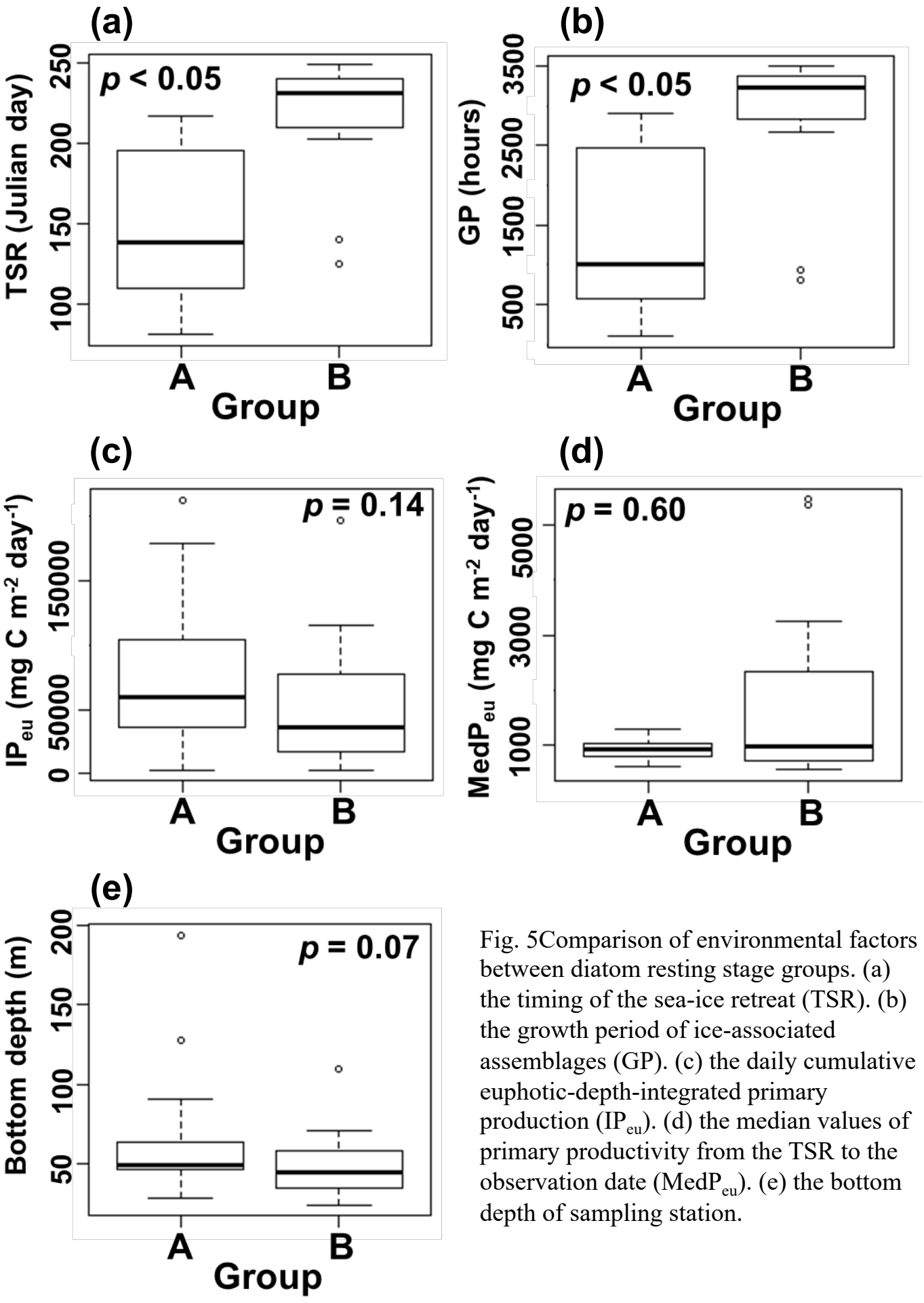

Fig. 5Comparison of environmental factors between diatom resting stage groups. (a) the timing of the sea-ice retreat (TSR). (b) the growth period of ice-associated assemblages (GP). (c) the daily cumulative euphotic-depth-integrated primary production (IP_{eu}). (d) the median values of primary productivity from the TSR to the observation date ($MedP_{eu}$). (e) the bottom depth of sampling station.

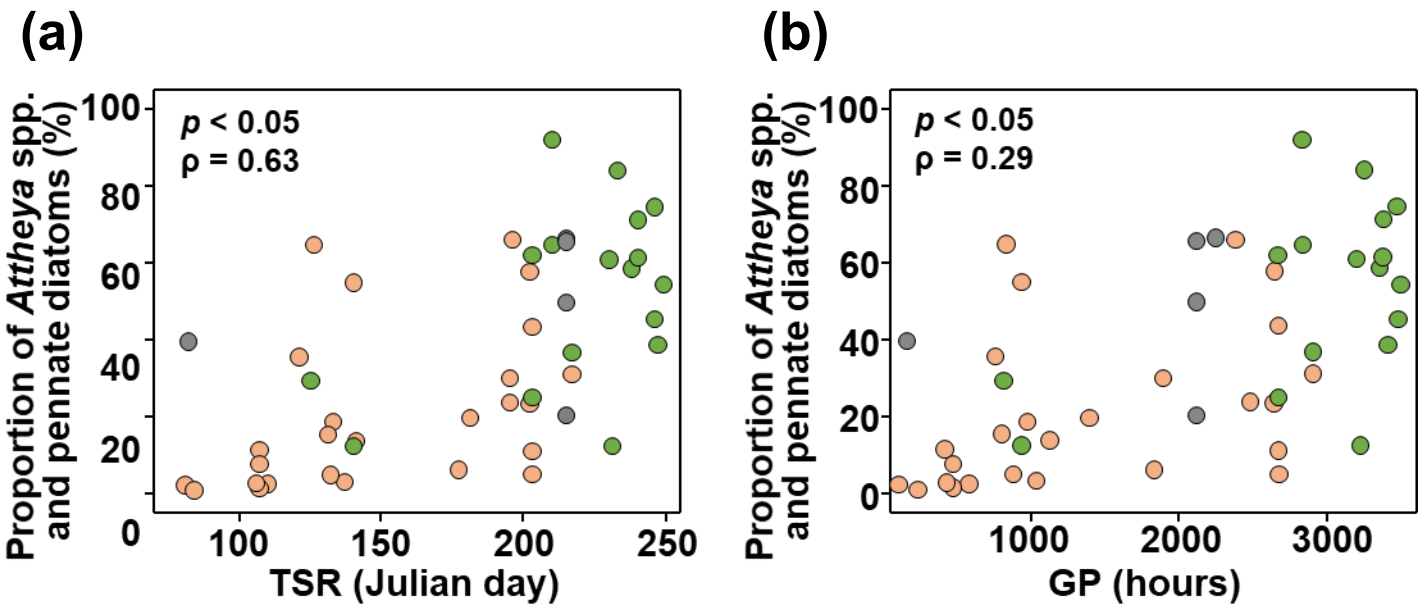

Fig. 6. Relationships between the proportion of the ice-associated species (*Attheya* spp. and pennate diatoms) in MPN and the TSR (a), and the GP (b). Each color indicate the diatom groups (pink: group A, green: group B, and gray: out groups).

Table 1. Locations of sediment sampling stations in the Bering, Chukchi, and Beaufort Seas from July to November in 2018. In sample type column, "core" and "Van Veen" indicate that the samples were collected by multiple corer and Van Veen grab sampler, respectively. The timing of sea ice retreat (TSR) indicates the last date when the sea ice concentration falls below 20%, prior to observed annual sea ice minimum across the study region during summer. IP_{eu} and $MedP_{eu}$ indicate daily integrated value and median value of primary production from TSR to the date of the *in situ* sediment sampling was conducted. The growth period of the ice-associated assemblages (GP) indicates the integrated daylength during the periods with SIC > 20% after the daylight hours exceed 10 hours.

Cruise	Station	Date (Julian day)	Latitude (°N)	Longitude (°W)	Bottom depth (m)	Sample Type	TSR (Julian day)	IP_{eu} (mg C m^{-2} day^{-1})	$MedP_{eu}$ (mg C m^{-2} day^{-1})	GP (hours)
Oshoro-maru C056	OS4	2018/7/2 (183)	63.15	173.83	75	Core	2018/3/23 (82)	80253.9	831.4	103.2
	OS6	2018/7/3 (184)	62.88	172.16	55	Core	2018/3/23 (82)	56305.7	554.5	158.4
	OS8	2018/7/3 (184)	62.49	170.00	37	Core	2018/3/24 (83)	77752.8	791.7	234.2
	OS14	2018/7/5 (186)	64.51	170.87	46	Core	2018/3/25 (84)	66311.6	924.2	414.7
	OS19	2018/7/6 (187)	64.51	166.51	28	Core	2018/4/24 (114)	39181.0	921.5	755.1
	OS20	2018/7/6 (187)	65.08	168.00	46	Core	2018/4/18 (108)	32002.1	777.2	581.4
	OS22	2018/7/7 (188)	65.07	169.70	51	Core	2018/4/17 (107)	106377.2	1300.4	469.0
	OS30	2018/7/11 (192)	66.73	168.96	42	Core	2018/4/24 (114)	59460.1	1030.9	1033.1
Healy 1801	DBO2-1	2018/8/9 (221)	64.67	169.93	48	Van Veen	2018/4/16 (106)	104868.8	840.7	427.2
	DBO2-4	2018/8/9 (221)	64.96	169.90	49	Van Veen	2018/4/17 (107)	143193.9	1094.8	469.0
	DBO3-6	2018/8/10 (222)	67.90	168.25	59	Core	2018/5/20 (140)	95858.0	1157.3	935.9
	DBO3-7	2018/8/11 (223)	67.79	168.60	51	Core	2018/5/21 (141)	104109.1	1276.0	935.1
	IC-3	2018/8/13 (225)	71.60	165.30	43	Van Veen	2018/6/26 (177)	32304.9	1008.3	1829.9
	IC-8	2018/8/14 (226)	70.97	163.56	46	Van Veen	2018/6/29 (180)	48394.7	1229.5	1391.3
	DBO4-2	2018/8/15 (227)	71.22	161.29	50	Core	2018/7/14 (195)	17824.0	886.5	1891.3
	DBO4-4	2018/8/15 (227)	71.48	161.50	49	Core	2018/7/15 (196)	15406.3	797.0	2377.8
	DBO4-5	2018/8/15 (227)	71.61	161.62	47	Core	2018/7/16 (197)	19747.3	924.1	2477.9
	DBO5-9	2018/8/17 (229)	71.58	157.82	66	Van Veen	2018/7/27 (208)	2915.4	751.2	2667.8
	DBO5-10	2018/8/17 (229)	71.63	157.90	64	Core	2018/7/26 (207)	2813.1	693.9	2669.9
	LB-11	2018/8/22 (234)	70.06	167.66	50	Van Veen	2018/5/13 (133)	95614.2	960.7	973.8
	LB-9	2018/8/23 (235)	69.88	166.82	47	Van Veen	2018/5/12 (132)	105276.1	993.8	877.1
	LB-7	2018/8/23 (235)	69.68	166.09	42	Van Veen	2018/5/12 (132)	96511.2	966.2	800.6

Healy 1803	DBO6-1	2018/10/30	(303)	71.16	152.26	32	Van Veen	2018/8/9	(221)	42213.8	5355.0	2824.9
	DBO6-3	2018/10/30	(303)	71.25	152.17	48	Van Veen	2018/8/8	(220)	55326.5	2401.6	2829.3
	DBO6-5	2018/10/30	(303)	71.34	152.10	71	Van Veen	2018/8/27	(239)	63070.1	1143.7	2899.2
	DBO6-7	2018/10/31	(304)	71.42	152.04	194	Van Veen	2018/8/28	(240)	52153.7	1024.0	2902.0
	PRB-1	2018/11/2	(306)	70.69	148.44	26	Van Veen	2018/8/21	(233)	—	—	3347.2
	PRB-2	2018/11/2	(306)	70.77	148.33	35	Van Veen	2018/8/24	(236)	17622.4	2275.3	3465.0
	PRB-4	2018/11/2	(306)	70.90	148.14	45	Van Veen	2018/9/3	(246)	16083.4	559.4	3405.6
	PRB-7	2018/11/2	(306)	71.02	147.98	58	Van Veen	2018/9/4	(247)	19897.2	751.8	3490.4
	MCK-1	2018/11/4	(308)	69.82	139.61	38	Van Veen	2018/8/22	(234)	40557.1	596.0	2240.4
	MCK-2	2018/11/4	(308)	69.90	139.49	44	Van Veen	2018/8/4	(216)	47209.6	792.0	2111.3
	MCK-3	2018/11/4	(308)	69.94	139.39	55	Van Veen	2018/8/1	(213)	47343.2	759.2	2113.9
	MCK-4	2018/11/4	(308)	69.97	139.30	60	Van Veen	2018/7/30	(211)	46782.5	753.7	2113.9
	KTO-2	2018/11/5	(309)	70.28	143.93	38	Van Veen	2018/8/22	(234)	30870.8	963.7	3191.8
	KTO-3	2018/11/5	(309)	70.37	143.79	48	Van Veen	2018/8/22	(234)	14101.3	564.3	3247.5
	KTO-5	2018/11/5	(309)	70.56	143.61	110	Van Veen	2018/8/18	(230)	13958.0	601.1	3221.7
	PRW-1	2018/11/7	(311)	70.68	148.91	24	Van Veen	2018/8/12	(224)	115525.9	5453.4	3369.1
	PRW-4	2018/11/7	(311)	70.82	148.84	33	Van Veen	2018/8/25	(237)	76570.9	3243.0	3373.2
	PRW-7	2018/11/7	(311)	70.95	148.78	38	Van Veen	2018/9/1	(244)	26140.8	709.0	3474.0
	DBO5-1	2018/11/14	(318)	71.25	157.13	47	Van Veen	2018/7/19	(200)	79117.8	839.1	2661.3
	DBO5-3	2018/11/41	(318)	71.33	157.31	91	Van Veen	2018/7/20	(201)	59407.8	903.6	2637.3
	DBO5-5	2018/11/14	(318)	71.41	157.49	128	Van Veen	2018/7/25	(206)	44093.7	745.2	2639.4
	DBO5-7	2018/11/14	(318)	71.50	157.66	85	Van Veen	2018/7/29	(210)	35765.2	676.0	2667.8
	DBO5-9	2018/11/14	(318)	71.58	157.83	66	Van Veen	2018/7/27	(208)	35857.3	620.0	2667.8
	DBO3-1	2018/11/15	(319)	68.31	166.92	35	Van Veen	2018/4/26	(116)	196800.9	1013.0	812.4
	DBO3-5	2018/11/15	(319)	68.01	167.88	54	Van Veen	2018/5/5	(125)	212878.6	1053.2	828.9
	DBO3-8	2018/11/15	(319)	67.67	168.95	50	Van Veen	2018/5/31	(151)	179194.6	1012.5	1124.6